Reduced parenchymal cerebral blood flow is associated with greater progression of brain atrophy: the SMART-MR study

Ghaznawi, R.; Zwartbol, M.H.T.; Zuithoff, N.P.A.; Bresser, J. de; Hendrikse, J.; Geerlings, M.I.; UCC-SMART Study Grp

Original Article

JCBFM

Journal of Cerebral Blood Flow & Metabolism
2021, Vol. 41(6) 1229–1239

DOI: 10.1177/0271678X20948614
journals.sagepub.com/home/jcbfm


Reduced parenchymal cerebral blood flow is associated with greater progression of brain atrophy: The SMART-MR study

Rashid Ghaznawi[1,2], Maarten HT Zwartbol[1], Nicolaas PA Zuithoff[2], Jeroen de Bresser[3], Jeroen Hendrikse[1] and Mirjam I Geerlings[2]; on behalf of the UCC-SMART Study Group*

Abstract

Global cerebral hypoperfusion may be involved in the aetiology of brain atrophy; however, long-term longitudinal studies on this relationship are lacking. We examined whether reduced cerebral blood flow was associated with greater progression of brain atrophy. Data of 1165 patients (61 ± 10 years) from the SMART-MR study, a prospective cohort study of patients with arterial disease, were used of whom 689 participated after 4 years and 297 again after 12 years. Attrition was substantial. Total brain volume and total cerebral blood flow were obtained from magnetic resonance imaging scans and expressed as brain parenchymal fraction (BPF) and parenchymal cerebral blood flow (pCBF). Mean decrease in BPF per year was 0.22% total intracranial volume (95% CI: –0.23 to –0.21). Mean decrease in pCBF per year was 0.24 ml/min per 100 ml brain volume (95% CI: –0.29 to –0.20). Using linear mixed models, lower pCBF at baseline was associated with a greater decrease in BPF over time ($p = 0.01$). Lower baseline BPF, however, was not associated with a greater decrease in pCBF ($p = 0.43$). These findings indicate that reduced cerebral blood flow is associated with greater progression of brain atrophy and provide further support for a role of cerebral blood flow in the process of neurodegeneration.

Keywords

Cerebral blood flow, brain atrophy, magnetic resonance imaging, cohort studies, epidemiology

Received 3 February 2020; Revised 5 July 2020; Accepted 12 July 2020

Introduction

Brain atrophy is a common finding on magnetic resonance imaging (MRI) in older individuals and individuals with manifest arterial disease.[1–3] Although brain atrophy occurs with normal ageing, previous studies have demonstrated that accelerated brain atrophy is associated with cognitive decline and dementia.[4–8] The underlying causes that can lead to progression of brain atrophy, however, remain largely unknown.[9]

Reduced cerebral blood flow has been postulated as a possible risk factor for brain tissue loss.[2,10–13] In physiological conditions, cerebral blood flow is regulated by the cerebral vasculature in order to maintain an adequate delivery of oxygen and nutrients to

[1]Department of Radiology, University Medical Center Utrecht and Utrecht University, Utrecht, the Netherlands
[2]Julius Center for Health Sciences and Primary Care, University Medical Center Utrecht and Utrecht University, Utrecht, the Netherlands
[3]Department of Radiology, Leiden University Medical Center, Leiden, the Netherlands

*Listed in the Acknowledgements section.

Corresponding author:
Mirjam I Geerlings, Julius Center for Health Sciences and Primary Care, University Medical Center Utrecht, PO Box 85500, Stratenum 6.131, 3508 GA Utrecht, the Netherlands.
Email: m.geerlings@umcutrecht.nl

the brain.[14] Failure of these mechanisms can lead to a reduced cerebral blood flow, which has been associated with mortality and an increased risk of dementia in large cohort studies.[15,16] Whether these relationships are mediated by progression of brain atrophy is not known as few studies have reported on the relationship between cerebral blood flow and brain atrophy.[2,10–12] In addition, there is some evidence to suggest that the relationship between cerebral blood flow and brain atrophy may be bidirectional, such that smaller brain volumes are a risk factor for greater decline in cerebral blood flow.[11] Examining the long-term longitudinal relationship between cerebral blood flow and brain atrophy is of importance as cerebral blood flow can be modified and may pose a potential target for future prevention strategies of brain atrophy and dementia.[17–19]

In the current study, we examined the longitudinal relationship between cerebral blood flow and brain atrophy in a large cohort of patients with manifest arterial disease over 12 years of follow-up.

Methods

Study population

Data from the Second Manifestations of ARTerial disease-Magnetic Resonance (SMART-MR) study, a prospective cohort study at the University Medical Center Utrecht with the aim to investigate risk factors and consequences of brain changes on MRI in patients with symptomatic arterial disease, were used.[20] Between 2001 and 2005, 1309 middle-aged and older adult individuals newly referred to the University Medical Center Utrecht for treatment of symptomatic atherosclerotic disease (manifest coronary artery disease (59%), cerebrovascular disease (23%), peripheral arterial disease (22%) or abdominal aortic aneurysm (9%)) were included for baseline measurements, including a 1.5 T brain MRI. Presence of neurodegenerative disease was not considered an exclusion criterion. Of these, 754 persons had follow-up measurements 4 years later between January 2006 and May 2009. During a 1 day visit to our medical centre, a physical examination, ultrasonography of the carotid arteries to measure the intima-media thickness (mm), blood and urine samplings, neuropsychological assessment and a 1.5 T brain MRI scan were performed. The height and weight were measured, and the body mass index (BMI) (kg/m^2) was calculated. Questionnaires were used for the assessment of demographics, risk factors, medical history, medication use and cognitive and physical functioning. Since November 2013, all patients alive were invited for a second follow-up, including a 1.5 T brain MRI, of which 329 persons had second follow-up measurements between November 2013 and October 2017. A flowchart of the SMART-MR study is shown in Figure 1.

The SMART-MR study was approved by the medical ethics committee of the University Medical Center Utrecht according to the guidelines of the Declaration of Helsinki of 1975, and written informed consent was obtained from all patients.

Vascular risk factors

At baseline, age, sex, smoking habits and alcohol intake were assessed with questionnaires. Height and weight were measured, and the BMI was calculated (kg/m^2). Systolic blood pressure (SBP) (mmHg) and diastolic blood pressure (DBP) (mmHg) were measured three times with a sphygmomanometer, and the average of these measures was calculated. Hypertension was defined as a mean SBP of >160 mmHg, a mean DBP of >95 mmHg or self-reported use of antihypertensive drugs. An overnight fasting venous blood sample was taken to determine glucose and lipids. Diabetes mellitus was defined as fasting serum glucose levels of ≥ 7.0 mmol/l, and/or use of glucose-lowering medication, and/or a known history of diabetes. Ultrasonography was performed with a 10 MHz linear-array transducer (ATL Ultramark 9), and the degree of the carotid artery stenosis at both sides was assessed with colour Doppler-assisted duplex scanning. The severity of carotid artery stenosis was evaluated on the basis of blood flow velocity patterns, and the greatest stenosis observed on the right or the left side of the common or internal carotid artery was taken to determine the severity of carotid artery disease. Carotid artery stenosis $\geq 70\%$ was defined as peak systolic velocity >210 cm/s.[21]

MRI protocol

MR imaging of the brain was performed on a 1.5 T whole-body system (Gyroscan ACS-NT, Philips Medical Systems, Best, the Netherlands) using a standardized scan protocol.[20] Transversal T1-weighted [repetition time (TR) = 235 ms; echo time (TE) = 2 ms], T2-weighted [TR = 2200 ms; TE = 11 ms], fluid-attenuated inversion recovery (FLAIR) [TR = 6000 m; TE = 100 ms; inversion time (TI) = 2000 ms] and T1-weighted inversion recovery images [TR = 2900 ms; TE = 22 ms; TI = 410 ms] were acquired with a voxel size of $1.0 \times 1.0 \times 4.0$ mm^3 and contiguous slices. For cerebral blood flow measurements, a two-dimensional phase-contrast section was positioned at the level of the skull base to measure the volume flow in the basilar artery and in the internal carotid arteries on the basis of a localizer MR angiographic slab in the sagittal plane.[22] The two-dimensional phase-contrast section

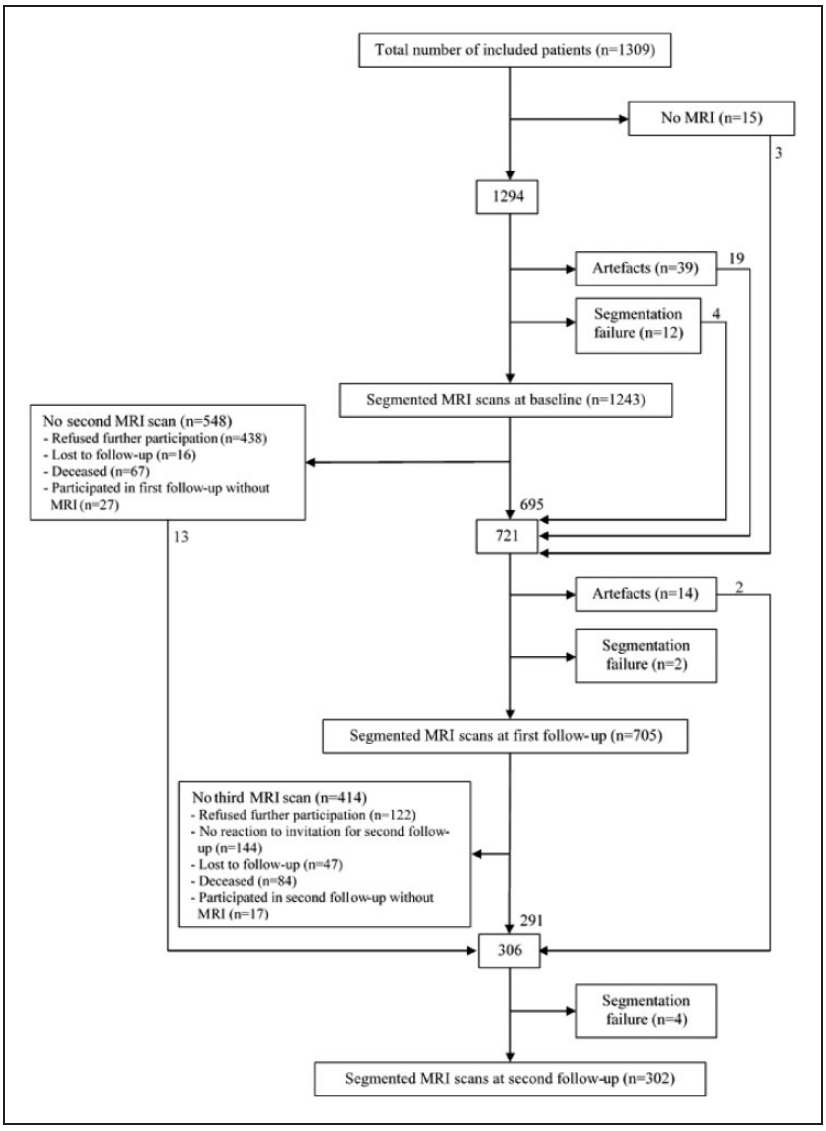

Figure 1. MRI participation flowchart of the SMART-MR study. Numbers in the boxes represent the numbers of patients who underwent a 1.5 T MRI at each time point.
MRI: magnetic resonance imaging.

was positioned through the basilar artery and the internal carotid arteries (TR/TE, 16/9 ms; flip angle 7.5°; field of view 250 × 250 mm; matrix size 256 × 256; slice thickness 5.0 mm; eight acquired signals; velocity sensitivity 100 cm/s).

Cerebral blood flow measurements

Phase-contrast MR angiography was used to measure total cerebral blood flow, as this method has been demonstrated to be a fast, reproducible and noninvasive method to measure total cerebral blood flow in large cohorts.[23,24] Previous studies established that phase-contrast MR angiography correlates well with arterial spin-labelled perfusion MRI, although estimates tend to be somewhat higher and more variable than arterial spin-labelled perfusion MRI.[25] Post-processing of the flow measurements was performed by investigators blinded to patient characteristics. The flow through the basilar and internal carotid arteries was summed to calculate the total cerebral blood flow. Total cerebral blood flow was expressed per 100 ml brain parenchymal volume to obtain parenchymal cerebral blood flow (pCBF).[16] Parenchymal CBF was measured at baseline, and at the first and second follow-up visits.

Brain volume measurements

White matter hyperintensity (WMH) volumes and brain volumes were obtained using the *k*-nearest

neighbour (kNN) automated segmentation programme on the T1-weighted, FLAIR and T1-weighted inversion recovery sequences of the MRI scans.[26] The kNN segmentation method has been shown to be suitable for detecting longitudinal brain volume changes.[20,27] All WMH segmentations were visually checked by an investigator (RG) using an image processing framework (MeVisLab 2.7.1., MeVis Medical Solutions AG, Bremen, Germany) to ensure that brain infarcts were correctly removed from the WMH segmentations. Incorrectly segmented voxels were added to the correct segmentation volumes using the image processing framework. Periventricular WMH were defined as lesions $\leq$1 cm of the lateral ventricles and deep WMH were defined as lesions that were located $>$1 cm of the lateral ventricles. Total brain volume was calculated by summing the volumes of grey matter, white matter, total WMH and, if present, the volumes of brain infarcts. Total intracranial volume (ICV) was calculated by summing the total brain volume and the volume of the cerebrospinal fluid. Total brain volume was normalized for ICV and expressed as brain parenchymal fraction (BPF). Brain volumes were measured at baseline, and at the first and second follow-up visits.

Brain infarcts

Brain infarcts were visually rated by a neuroradiologist blinded to patient characteristics on the T1-weighted, T2-weighted and FLAIR images of the MRI scans. Lacunes were defined as focal lesions between 3 and 15 mm according to the STRIVE criteria,[28] whereas non-lacunar lesions were divided into large infarcts (i.e. cortical infarcts and subcortical infarcts not involving the cerebral cortex) and those located in the cerebellum or brain stem.

Study sample

At baseline, 1165 patients had both pCBF and BPF measurements, whereas this was the case for 689 and 297 patients at the first and second follow-ups, respectively. The study sample included patients with consecutive and non-consecutive pCBF and/or BPF measurements.

Statistical analysis

Baseline characteristics of patients with BPF and pCBF measurements at baseline (n = 1165) were reported as means or percentages where applicable. Baseline characteristics of patients with follow-up measurements and those without were compared using an independent samples t-test and Chi square test for continuous and dichotomous variables, respectively.

Linear mixed models were used to analyze change in BPF and change in pCBF over time.[29,30] As the time intervals between MRI measurements differed between patients, the age of patients at the MRI measurements was chosen as the time variable. Age was centred on 61 years, the mean value at which the first MRI measurement was performed. BPF and pCBF were analyzed per standard deviation decrease. To minimize the risk of bias due to complete case analysis, chained equations imputation was performed on missing covariates to generate 10 imputed datasets using SPSS 25.0 (Chicago, IL, USA).[31] Statistical analyses were performed on these datasets, and pooled results were presented. In chained equations imputation, linear and logistic regressions are used to impute continuous and categorical covariates, respectively, using other covariates as predictors.[31]

First, we modelled longitudinal measurements of BPF (dependent variable) with pCBF as time-varying predictor, with age at time of MRI as the time-scale and adjusted for baseline age and sex. In a second model, we additionally adjusted for large infarcts, lacunes and WMH volume on MRI, DBP, hypertension, carotid stenosis $\geq$70%, BMI and smoking pack years at baseline. To determine whether baseline pCBF was a risk factor for subsequent BPF decline, we modelled change in BPF with baseline pCBF. Baseline pCBF, time, baseline age, sex and the interaction between baseline pCBF and time were entered in a model. Next, we additionally adjusted for large infarcts, lacunes and WMH volume on MRI, hypertension, diabetes mellitus, carotid stenosis $\geq$70%, BMI and smoking pack years at baseline.

Second, we modelled longitudinal measurements of pCBF (dependent variable) with BPF as time-varying predictor with age at time of MRI as the time-scale and adjusted for baseline age and sex. In the second model, we additionally adjusted for large infarcts, lacunes and WMH volume on MRI, hypertension, diabetes mellitus, carotid stenosis $\geq$70%, BMI and smoking pack years at baseline. To determine whether baseline BPF was a risk factor for subsequent pCBF decline, we modelled change in pCBF with baseline BPF. Next, we additionally adjusted for large infarcts, lacunes and WMH volume on MRI, hypertension, diabetes mellitus, carotid stenosis $\geq$70%, BMI and smoking pack years at baseline.

In all models, a random intercept and random slope with time were assumed, meaning that the models accounted for individual variation in the starting level of BPF or pCBF (intercept) and in change of BPF or pCBF over time (slope), respectively. Adequacy of all models was determined by examining the residuals for homoscedasticity and normality.[32] We concluded that model assumptions were adequately met. Statistical

significance was set at $p \leq 0.05$. Due to the exploratory nature of the analyses, no adjustment of p values was made for multiple comparisons. SAS 9.4 (SAS Institute, Cary, NC, USA) and SPSS 25.0 (Chicago, IL, USA) were used to perform the statistical analyses.

As sensitivity analyses, we assumed a fixed slope with time and repeated the analyses with baseline pCBF as predictor and change in BPF as outcome, and with baseline BPF as predictor and change in pCBF as outcome. In addition, to examine whether multiple imputation affected the results, we repeated the analyses in patients without missing data (i.e. complete case analysis). Lastly, to examine the effect of attrition on the results of the longitudinal analyses, we hypothesized that dropout due to death may represent a form of informative dropout. We examined the effect of dropout due to death on the results of the linear mixed models using a joint modelling approach that includes a time-to-event submodel.[33] For the time-to-event submodel, data on occurrence of death and survival times were obtained from questionnaires that patients received biannually. Acquisition of data relating to occurrence of death and survival times is described in detail elsewhere.[34] The JM package for R version 3.6.3 (R Core Team, 2019) was used to perform the joint model analysis.[33]

Results

Baseline characteristics of the study sample (n = 1165) are shown in Table 1. The mean age at baseline was 61 ± 10 years and 80% were male. Mean pCBF was 51.4 ± 10.6 ml/min per 100 ml brain volume. Mean time between baseline and first follow-up measurements for patients with available pCBF and BPF data (n = 689) was 3.9 ± 0.4 years (range 2.9–5.8 years). Mean time between the first follow-up and second follow-up measurements for patients with available pCBF and BPF data (n = 297) was 8.2 ± 0.4 years (range 7.3–9.5 years). Mean time between baseline and the second follow-up measurements was 12.0 ± 0.4 years (range 11.1–13.5 years) for patients with available pCBF and BPF data on the second follow-up (n = 297). Mean decrease in BPF per year for the study sample was 0.22% ICV (95% CI: –0.23 to –0.21). Mean decrease in pCBF per year was 0.24 ml/min per 100 ml brain volume (95% CI: –0.29 to –0.20). Patients with follow-up measurements (n = 754) were younger ($p < 0.001$), more often male ($p = 0.011$), had more often current alcohol use ($p = 0.001$), had less often hypertension ($p = 0.001$), diabetes mellitus ($p < 0.001$) and carotid artery stenosis ≥70% ($p = 0.04$), and had a greater BPF ($p < 0.001$) and smaller WMH volumes on MRI ($p < 0.001$) compared to patients without follow-up measurements (n = 555) (Table 2).

Table 1. Characteristics of the study population with available pCBF and BPF data at baseline (n = 1165).

Age, years	61 ± 10
Sex, % men	80.3
History of stroke, %	23.3
BMI, kg/m^2	27 ± 4
Smoking, pack years[a]	19 (0, 50)
Alcohol use, %	
Current	75.0
Former	8.7
Never	16.3
Hypertension, %	50.9
Diabetes mellitus, %	20.6
Carotid artery stenosis ≥70%, %	10.6
Infarcts on MRI, %	
Large	12.2
Cerebellar	4.0
Brainstem	2.9
Lacunes on MRI, %	18.5
WMH volumes on MRI, ml[a]	
Total	0.9 (0.2, 6.5)
Periventricular	0.6 (0.1, 4.2)
Deep	0.3 (0.0, 2.5)
BPF, % ICV	79.0 ± 2.9
pCBF, ml/min per 100 ml brain volume	51.4 ± 10.6

Note: Characteristics are presented as mean ± SD or %.
[a]Median (10th percentile, 90th percentile).
BMI: body mass index; BPF: brain parenchymal fraction; ICV: total intracranial volume; MRI: magnetic resonance imaging; pCBF: parenchymal cerebral blood flow; SD: standard deviation; WMH: white matter hyperintensity.

Time-varying pCBF as a predictor of time-varying BPF

Lower pCBF was associated with lower BPF at baseline and follow-up, adjusted for age and sex. Specifically, each standard deviation decrease in pCBF at a given time point was associated with an additional 0.10% ICV lower BPF at that given time point (95% CI: –0.17 to –0.04, $p = 0.001$). This relationship remained statistically significant after adjusting for large infarcts, lacunes and WMH volume on MRI, hypertension, diabetes mellitus, carotid stenosis ≥70%, BMI, alcohol use and smoking pack years at baseline (B = –0.09% ICV, 95% CI: –0.15 to –0.03, $p = 0.005$).

Baseline pCBF as a predictor of longitudinal BPF

Adjusted for age and sex, lower baseline pCBF was associated with greater subsequent decreases in BPF. Specifically, each standard deviation decrease in baseline pCBF was associated with an additional 0.01% ICV decrease per year in BPF (95% CI: –0.02 to

Table 2. Baseline characteristics of the study population (n = 1309) according to participation in follow-up visits.

	Patients with one or two follow-up visits (n = 754)	Patients without follow-up visits (n = 555)	*p* value
Age, years	58 ± 9	60 ± 11	<0.001
Sex, % men	82.1	76.4	0.011
History of stroke, %	23.7	22.2	0.503
BMI, kg/m^2	27 ± 4	27 ± 4	0.568
Smoking, pack years[a]	20 (0, 49)	17 (0, 53)	0.253[b]
Alcohol use, % current	79	70	0.001
Hypertension, %	47.9	57.3	0.001
Diabetes mellitus, %	16.3	27.1	<0.001
Carotid artery stenosis ≥70%, %	9.6	13.3	0.04
Infarcts on MRI, %			
Large	11.3	14.0	0.152
Cerebellar	3.8	4.5	0.528
Brainstem	2.7	3.2	0.490
Lacunes on MRI, %	17.3	20.7	0.117
WMH volumes on MRI, ml[a]			
Total	0.8 (0.2, 4.8)	1.1 (0.3, 8.8)	<0.001[b]
Periventricular	0.5 (0.1, 3.0)	0.8 (0.1, 5.7)	<0.001[b]
Deep	0.2 (0.0, 2.1)	0.3 (0.0, 3.6)	<0.001[b]
BPF, % ICV	79.3 ± 2.6	78.5 ± 3.2	<0.001
pCBF, ml/min per 100 ml brain volume	51.6 ± 10.4	51.0 ± 10.9	0.336

Note: Characteristics are presented as mean ± SD or %.[a]Median (10th percentile, 90th percentile).
[b]Natural log-transformed due to a non-normal distribution in the statistical analysis.
BMI: body mass index; BPF: brain parenchymal fraction; ICV: total intracranial volume; MRI: magnetic resonance imaging; pCBF: parenchymal cerebral blood flow; SD: standard deviation; WMH: white matter hyperintensity.

–0.004, $p = 0.004$) (Table 3). This relationship remained statistically significant after adjusting for large infarcts, lacunes and WMH volume on MRI, hypertension, diabetes mellitus, carotid stenosis ≥70%, BMI, alcohol use and smoking pack years at baseline (B = –0.01% ICV, 95% CI: –0.02 to –0.003, $p = 0.010$).

Time-varying BPF as a predictor of time-varying pCBF

Lower BPF was associated with lower pCBF at baseline and follow-up, adjusted for age and sex. Each standard deviation decrease in BPF at a given time point was associated with an additional 0.90 ml/min per 100 ml brain volume lower pCBF at that given time point (95% CI: –1.57 to –0.24, $p = 0.008$). The estimate attenuated and lost statistical significance after adjusting for large infarcts, lacunes and WMH volume on MRI, hypertension, diabetes mellitus, carotid stenosis ≥70%, BMI, alcohol use and smoking pack years at baseline (B = –0.58 ml/min per 100 ml brain volume, 95% CI: –1.28 to 0.12, $p = 0.104$).

Baseline BPF as a predictor of longitudinal pCBF

Adjusted for age and sex, lower baseline BPF was not associated with greater subsequent decreases in pCBF (B = 0.02 ml/min per 100 ml brain volume, 95% CI: –0.03 to 0.07, $p = 0.439$) (Table 4). This relationship did not change after adjusting for large infarcts, lacunes and WMH volume on MRI, hypertension, diabetes mellitus, carotid stenosis ≥70%, BMI, alcohol use and smoking pack years at baseline (B = 0.02 ml/min per 100 ml brain volume, 95% CI: –0.03 to 0.07, $p = 0.429$).

Sensitivity analyses

Lower baseline pCBF was associated with a greater subsequent decrease in BPF when assuming a fixed slope with time or when performing the analysis only in patients without missing data, adjusted for age, sex, large infarcts, lacunes and WMH volume on MRI, hypertension, diabetes mellitus, carotid stenosis ≥70%, BMI, alcohol use and smoking pack years at baseline (Supplementary Table 1 and Supplementary Table 2, respectively). Baseline BPF was not associated with change in pCBF over time when assuming a fixed slope with time or when performing the analysis only in patients without missing data.

A total of 167 patients (14%) died during the study. Accounting for dropout due to death, lower baseline pCBF was associated with a greater subsequent decline

Table 3. Results of the linear mixed model with BPF as dependent variable and baseline pCBF as independent variable.

	Model 1		Model 2	
	Estimate (95% CI)	*p* value	Estimate (95% CI)	*p* value
Intercept	78.50 (78.35 to 78.64)	<0.001	78.61 (77.71 to 79.51)	<0.001
Baseline pCBF[a]	–0.19 (–0.32 to –0.07)	0.002	–0.12 (–0.24 to 0.00)	0.051
Rate of change				
Time[b]	–0.24 (–0.25 to –0.22)	<0.001	–0.23 (–0.25 to –0.22)	<0.001
Time × baseline pCBF	–0.01 (–0.02 to –0.004)	0.004	–0.01 (–0.02 to –0.003)	0.010
Age[b]	–0.04 (–0.06 to –0.03)	<0.001	–0.05 (–0.07 to –0.04)	<0.001
Sex[c]	0.90 (0.59 to 1.21)	<0.001	0.86 (0.55 to 1.17)	<0.001
Large infarcts on MRI	–		–0.61 (–1.00 to –0.20)	0.003
Lacunes on MRI	–		–0.60 (–0.94 to –0.26)	<0.001
WMH volume on MRI[d]	–		–0.01 (–0.11 to 0.09)	0.836
Hypertension	–		–0.19 (–0.43 to 0.05)	0.117
Diabetes mellitus	–		–1.05 (–1.35 to –0.74)	<0.001
Carotid stenosis ≥70%	–		–0.17 (–0.61 to 0.27)	0.460
Body mass index	–		0.03 (–0.01 to 0.06)	0.109
Smoking pack years	–		–0.01 (–0.02 to –0.01)	<0.001
Alcohol use				
Current	–		0 (reference)	–
Former	–		–0.41 (–0.84 to 0.01)	0.056
Never	–		0.06 (–0.28 to 0.40)	0.728

Note: Estimates represent fixed effects of the linear mixed model with their 95% confidence intervals for a one unit increase of a continuous variable or presence of a dichotomous variable unless stated otherwise.

Model 1: adjusted for age and sex.

Model 2: additionally adjusted for large infarcts on MRI, lacunes on MRI, WMH volume on MRI, hypertension, diabetes mellitus, carotid stenosis ≥70%, body mass index, alcohol use and smoking pack years at baseline.

ICC model 1: 0.87; ICC model 2: 0.86; Marginal R^2 Model 1: 0.48; Conditional R^2 Model 1: 0.94; Marginal R^2 Model 2: 0.53; Conditional R^2 Model 2: 0.94.

[a]Per standard deviation decrease.

[b]Per year increase.

[c]Females vs. males.

[d]Natural log-transformed due to a non-normal distribution and normalized for total intracranial volume.

ICC: intra-class correlation coefficient; MRI: magnetic resonance imaging; pCBF: parenchymal cerebral blood flow; WMH: white matter hyperintensity.

in BPF (B = –0.02, 95% CI: –0.03 to –0.002, $p = 0.009$) in a joint model that included age, sex, large infarcts, lacunes, WMH volume, hypertension, diabetes mellitus, carotid stenosis ≥70%, BMI, alcohol use and smoking pack years at baseline as covariates in the linear mixed and time-to-event submodels.

Discussion

In this cohort of patients with manifest arterial disease, we observed that a reduced pCBF was associated with smaller total brain volumes, and that smaller total brain volumes were associated with reduced pCBF throughout the follow-up period of 12 years. Reduced pCBF at baseline was associated with a greater subsequent decline in BPF in a model that controlled for sex, cardiovascular risk factors, brain infarcts and small vessel disease. However, reduced BPF at baseline was not associated with a greater decline in pCBF.

Our finding that lower pCBF was associated with lower BPF at baseline and at follow-up is in line with previous cross-sectional studies that reported smaller total brain volumes in patients with reduced cerebral blood flow.[12,13,35] A study in patients with a history of arterial disease found a significant correlation between total cerebral blood flow measured using phase-contrast MR angiography and total brain volume.[13] Similarly, a smaller population-based study revealed that decreased total brain perfusion measured using arterial spin labelling MRI was associated with smaller total brain volumes.[12] A study comparing patients with Alzheimer's disease with age-matched controls showed that reduced total cerebral blood flow was associated with smaller total brain volumes only in patients with Alzheimer's disease, whereas this relationship was not found in the control group.[35] To our knowledge, only one previous study reported on the longitudinal relationship between cerebral blood flow and total brain

Table 4. Results of the linear mixed model with pCBF as dependent variable and baseline BPF as independent variable.

	Model 1		Model 2	
	Estimate (95% CI)	*p* value	Estimate (95% CI)	*p* value
Intercept	50.31 (49.57 to 51.06)	<0.001	51.56 (47.46 to 55.67)	<0.001
Baseline BPF[a]	–0.48 (–1.20 to 0.37)	0.185	–0.06 (–0.80 to 0.67)	0.868
Rate of change				
Time[b]	–0.35 (–0.45 to –0.26)	<0.001	–0.36 (–0.45 to –0.27)	<0.001
Time × baseline BPF	0.02 (–0.03 to 0.07)	0.439	0.02 (–0.03 to 0.07)	0.429
Age[b]	–0.18 (–0.30 to –0.07)	<0.001	–0.22 (–0.34 to –0.11)	<0.001
Sex[c]	3.56 (2.22 to 4.89)	<0.001	4.17 (2.78 to 5.55)	<0.001
Large infarcts on MRI	–		–1.40 (–3.17 to 0.37)	0.121
Lacunes on MRI	–		0.68 (–0.81 to 2.17)	0.371
WMH volume on MRI[d]	–		–0.50 (–0.97 to –0.04)	0.034
Hypertension	–		–1.32 (–2.39 to –0.24)	0.016
Diabetes mellitus	–		–0.36 (–1.74 to 1.02)	0.609
Carotid stenosis ≥70%	–		–4.98 (–6.88 to –3.08)	<0.001
Body mass index	–		–0.06 (–0.21 to 0.08)	0.410
Smoking pack years	–		0.02 (–0.01 to 0.04)	0.184
Alcohol use				
Current	–		0 (reference)	
Former	–		–1.28 (–3.21 to 0.64)	0.191
Never	–		0.45 (–1.05 to 1.96)	0.556

Note: Estimates represent fixed effects of the linear mixed model with their 95% confidence intervals for a one unit increase of a continuous variable or presence of a dichotomous variable unless stated otherwise.

Model 1: adjusted for age and sex.

Model 2: additionally adjusted for large infarcts on MRI, lacunes on MRI, WMH volume on MRI, hypertension, diabetes mellitus, carotid stenosis ≥70%, body mass index, alcohol use and smoking pack years at baseline.

ICC model 1: 0.54; ICC model 2: 0.52; Marginal R^2 Model 1: 0.27; Conditional R^2 Model 1: 0.65; Marginal R^2 Model 2: 0.33; Conditional R^2 Model 2: 0.65.

[a]Per standard deviation decrease.

[b]Per year increase.

[c]Females vs. males.

[d]Natural log-transformed due to a non-normal distribution and normalized for total intracranial volume.

BPF: brain parenchymal fraction; ICC: intra-class correlation coefficient; MRI: magnetic resonance imaging; WMH: white matter hyperintensity.

volume.[11] In this population-based cohort study, reduced total cerebral blood flow was associated with greater progression of brain atrophy only in older patients, whereas a smaller brain volume at baseline was associated with a steeper decrease in total cerebral blood flow in the whole population.[11] A direct comparison with the findings of the present study, however, is possible only to a limited extent due to the shorter follow-up period and the use of total cerebral blood flow instead of pCBF.

We found that reduced baseline pCBF was significantly associated with greater decline in BPF; however, the effect size was modest when taking into account the estimated mean annual decline in BPF. A number of remarks should be made with respect to this finding. First, the volumetric technique used in our study did not allow us to measure region-specific brain volume changes. Recent cross-sectional studies using arterial spin labelling and dynamic-susceptibility contrast MRI reported regional effects of reduced cerebral blood flow on specific brain volumes, predominantly the temporal lobes.[12,35,36] Similarly, the use of phase-contrast MR angiography did not allow us to measure region-specific cerebral blood flow. It is therefore possible that the association between pCBF and progression of brain atrophy in the present study reflects regional effects of cerebral blood flow on specific brain regions. Second, the longitudinal analysis included patients with multiple BPF measurements and these patients may represent a healthier group, which may have led to an underestimation of the association of pCBF with progression of brain atrophy. Nonetheless, the significant longitudinal relationship between pCBF and BPF in the present study supports a role of cerebral blood flow in the process of neurodegeneration and, from a clinical perspective,

strengthens the notion that cerebral blood flow could be a potential target for future prevention strategies of brain atrophy.[17–19]

In the present study, we chose a bidirectional modelling approach between pCBF and BPF for the following reasons. First, although experimental studies using animal models suggest that reduced cerebral blood flow may be a risk factor for brain tissue loss,[37] some studies hypothesized that smaller brain volumes may lead to reduced metabolic demand, which in turn may lead to a greater decrease in cerebral blood flow over time.[38] Second, a previous longitudinal study with a shorter follow-up period reported that smaller brain volumes at baseline were associated with a greater decline in cerebral blood flow.[11] The results of the present study, however, provide support for the notion that reduced pCBF is a risk factor for greater subsequent brain atrophy.

Strengths of the present study are the longitudinal design with pCBF and BPF measurements at three time points, the large sample size and the relatively long follow-up period. In addition, the detailed information on cardiovascular risk factors and cerebrovascular lesions allowed us to adjust for these possible confounders in the association between pCBF and BPF over time. Also, we used a statistical modelling approach that allowed patients to have a variable number of measurements and accounted for differences in time intervals between measurements.

Limitations are as follows: first, cerebral autoregulatory mechanisms to maintain adequate cerebral blood flow and cardiac output were not considered in this study, which is a major limitation. Second, as mentioned above, the volumetric technique used in our study did not allow us to measure region-specific brain volume changes and phase-contrast MR angiography did not allow region-specific assessment of blood flow, which is likely more sensitive in detecting associations with brain atrophy. Third, volumetry was performed on MRI sequences with a slice thickness of 4 mm instead of 1 mm, which is more sensitive in detecting brain volume changes. Fourth, our study sample consisted of mostly males with a relatively young age and a history of arterial disease, which may limit the generalizability of our results. Lastly, although the MRI scan protocol did not change throughout the study, each patient was not necessarily scanned using the exact same MRI scanner over time and scanner stability was not determined.

In conclusion, our findings demonstrate that reduced pCBF is independently associated with greater progression of brain atrophy in patients with manifest arterial disease. These findings provide further support for a role of cerebral blood flow in the process of neurodegeneration.

Funding

The author(s) disclosed receipt of the following financial support for the research, authorship, and/or publication of this article: Funding for this paper was received as part of a grant from the Netherlands Organization for Scientific Research-Medical Sciences (NWO-MW: project No. 904-65-095). This funding source had no role in the design, data collection, data analyses and data interpretation of the study or writing of the report. We also gratefully acknowledge the funding from the European Research Council under the European Union's Horizon 2020 Programme (H2020)/ERC grant agreement no. 637024 and no. 66681 (SVDs@target).

Acknowledgements

We gratefully acknowledge the contribution of the research nurses; R. van Petersen (data-manager); B. van Dinther (study manager) and the members of the Utrecht Cardiovascular Cohort-Second Manifestations of ARTerial disease-study group (UCC-SMART-study group): F.W. Asselbergs and H.M. Nathoe, Department of Cardiology; G.J. de Borst, Department of Vascular Surgery; M.L. Bots and M.I. Geerlings, Julius Center for Health Sciences and Primary Care; M.H. Emmelot, Department of Geriatrics; P. A. de Jong and T. Leiner, Department of Radiology; A.T. Lely, Department of Obstetrics/Gynaecology; N.P. van der Kaaij, Department of Cardiothoracic Surgery; L.J. Kappelle and Y. Ruigrok, Department of Neurology; M.C. Verhaar, Department of Nephrology, F.L.J. Visseren (chair) and J. Westerink, Department of Vascular Medicine, University Medical Center Utrecht and Utrecht University. We also gratefully acknowledge the assistance and support of Dr. JMJ Vonk in the joint model analysis.

Declaration of conflicting interests

The author(s) declared no potential conflicts of interest with respect to the research, authorship, and/or publication of this article.

Authors' contributions

RG: literature search, figures, data collection, MR image processing, data analysis, data interpretation and writing; PZ: data analysis, data interpretation and critically reviewed the manuscript; JB: data interpretation and critically reviewed the manuscript; MZ: MR image processing and analysis, critically reviewed the manuscript; JH: critically reviewed the manuscript; MIG: study design, data analysis and interpretation, and critically reviewed the manuscript.

ORCID iDs

Rashid Ghaznawi https://orcid.org/0000-0002-6616-5276
Maarten HT Zwartbol https://orcid.org/0000-0001-5779-3150

Supplementary material

Supplementary material for this paper is available online.

References

1. Resnick SM, Pham DL, Kraut MA, et al. Longitudinal magnetic resonance imaging studies of older adults: a shrinking brain. *J Neurosci* 2003; 23: 3295–3301.
2. Appelman AP, van der Graaf Y, Vincken KL, et al. Total cerebral blood flow, white matter lesions and brain atrophy: the SMART-MR study. *J Cereb Blood Flow Metab* 2008; 28: 633–639.
3. Enzinger C, Fazekas F, Matthews PM, et al. Risk factors for progression of brain atrophy in aging: six-year follow-up of normal subjects. *Neurology* 2005; 64: 1704–1711.
4. Jack CR Jr., Shiung MM, Gunter JL, et al. Comparison of different MRI brain atrophy rate measures with clinical disease progression in AD. *Neurology* 2004; 62: 591–600.
5. Jack CR Jr., Shiung MM, Weigand SD, et al. Brain atrophy rates predict subsequent clinical conversion in normal elderly and amnestic MCI. *Neurology* 2005; 65: 1227–1231.
6. Kramer JH, Mungas D, Reed BR, et al. Longitudinal MRI and cognitive change in healthy elderly. *Neuropsychology* 2007; 21: 412–418.
7. Silbert LC, Quinn JF, Moore MM, et al. Changes in premorbid brain volume predict Alzheimer's disease pathology. *Neurology* 2003; 61: 487–492.
8. Fox NC, Scahill RI, Crum WR, et al. Correlation between rates of brain atrophy and cognitive decline in AD. *Neurology* 1999; 52: 1687–1689.
9. Raz N and Kennedy K. A systems approach to age-related change: neuroanatomical changes, their modifiers, and cognitive correlates. In: Jagust W and D'Esposito M (eds) *Imaging the Aging Brain*. 1st ed. Oxford: Oxford University Press, 2009, pp.43–70.
10. Kitagawa Y, Meyer JS, Tanahashi N, et al. Cerebral blood flow and brain atrophy correlated by xenon contrast CT scanning. *Comput Radiol* 1985; 9: 331–340.
11. Zonneveld HI, Loehrer EA, Hofman A, et al. The bidirectional association between reduced cerebral blood flow and brain atrophy in the general population. *J Cereb Blood Flow Metab* 2015; 35: 1882–1887.
12. Alosco ML, Gunstad J, Jerskey BA, et al. The adverse effects of reduced cerebral perfusion on cognition and brain structure in older adults with cardiovascular disease. *Brain Behav* 2013; 3: 626–636.
13. van Es AC, van der Grond J, ten Dam VH, et al. Associations between total cerebral blood flow and age related changes of the brain. *PLoS One* 2010; 5: e9825.
14. van Beek AH, Claassen JA, Rikkert MG, et al. Cerebral autoregulation: an overview of current concepts and methodology with special focus on the elderly. *J Cereb Blood Flow Metab* 2008; 28: 1071–1085.
15. Sabayan B, van der Grond J, Westendorp RG, et al. Total cerebral blood flow and mortality in old age: a 12-year follow-up study. *Neurology* 2013; 81: 1922–1929.
16. Wolters FJ, Zonneveld HI, Hofman A, et al. Cerebral perfusion and the risk of dementia: a population-based study. *Circulation* 2017; 136: 719–728.
17. Espeland MA, Luchsinger JA, Neiberg RH, et al. Long term effect of intensive lifestyle intervention on cerebral blood flow. *J Am Geriatr Soc* 2018; 66: 120–126.
18. Muller M, van der Graaf Y, Visseren FL, et al. Hypertension and longitudinal changes in cerebral blood flow: the SMART-MR study. *Ann Neurol* 2012; 71: 825–833.
19. de la Torre JC. Cerebral perfusion enhancing interventions: a new strategy for the prevention of Alzheimer dementia. *Brain Pathol* 2016; 26: 618–631.
20. Geerlings MI, Appelman AP, Vincken KL, et al. Brain volumes and cerebrovascular lesions on MRI in patients with atherosclerotic disease. The SMART-MR study. *Atherosclerosis* 2010; 210: 130–136.
21. Muller M, van der Graaf Y, Algra A, et al. Carotid atherosclerosis and progression of brain atrophy: the SMART-MR study. *Ann Neurol* 2011; 70: 237–244.
22. Bakker CJ, Kouwenhoven M, Hartkamp MJ, et al. Accuracy and precision of time-averaged flow as measured by nontriggered 2D phase-contrast MR angiography, a phantom evaluation. *Magn Reson Imaging* 1995; 13: 959–965.
23. Vernooij MW, van der Lugt A, Ikram MA, et al. Total cerebral blood flow and total brain perfusion in the general population: the Rotterdam Scan Study. *J Cereb Blood Flow Metab* 2008; 28: 412–419.
24. Spilt A, Box FM, van der Geest RJ, et al. Reproducibility of total cerebral blood flow measurements using phase contrast magnetic resonance imaging. *J Magn Reson Imaging* 2002; 16: 1–5.
25. Dolui S, Wang Z, Wang DJJ, et al. Comparison of non-invasive MRI measurements of cerebral blood flow in a large multisite cohort. *J Cereb Blood Flow Metab* 2016; 36: 1244–1256.
26. Anbeek P, Vincken KL, van Bochove GS, et al. Probabilistic segmentation of brain tissue in MR imaging. *Neuroimage* 2005; 27: 795–804.
27. de Boer R, Vrooman HA, Ikram MA, et al. Accuracy and reproducibility study of automatic MRI brain tissue segmentation methods. *Neuroimage* 2010; 51: 1047–1056.
28. Wardlaw JM, Smith EE, Biessels GJ, et al. Neuroimaging standards for research into small vessel disease and its contribution to ageing and neurodegeneration. *Lancet Neurol* 2013; 12: 822–838.
29. Carmichael O, Schwarz C, Drucker D, et al. Longitudinal changes in white matter disease and cognition in the first year of the Alzheimer disease neuroimaging initiative. *Arch Neurol* 2010; 67: 1370–1378.
30. Benedictus MR, Leeuwis AE, Binnewijzend MA, et al. Lower cerebral blood flow is associated with faster cognitive decline in Alzheimer's disease. *Eur Radiol* 2017; 27: 1169–1175.
31. White IR, Royston P and Wood AM. Multiple imputation using chained equations: issues and guidance for practice. *Stat Med* 2011; 30: 377–399.
32. Singer JD and Willett JB. *Applied longitudinal data analysis: modeling change and event occurrence*. Oxford: Oxford University Press, 2003.

33. Rizopoulos D. JM: an R package for the joint modelling of longitudinal and time-to-event data. *Journal of Statistical Software* 2010; 35: 1–33.
34. Goessens BM, Visseren FL, Kappelle LJ, et al. Asymptomatic carotid artery stenosis and the risk of new vascular events in patients with manifest arterial disease: the SMART study. *Stroke* 2007; 38: 1470–1475.
35. Benedictus MR, Binnewijzend MAA, Kuijer JPA, et al. Brain volume and white matter hyperintensities as determinants of cerebral blood flow in Alzheimer's disease. *Neurobiol Aging* 2014; 35: 2665–2670.
36. Wirth M, Pichet Binette A, Brunecker P, et al. Divergent regional patterns of cerebral hypoperfusion and gray matter atrophy in mild cognitive impairment patients. *J Cereb Blood Flow Metab* 2017; 37: 814–824.
37. Washida K, Hattori Y and Ihara M. Animal models of chronic cerebral hypoperfusion: from mouse to primate. *Int J Mol Sci* 2019; 20: 6176.
38. Shaw TG, Mortel KF, Meyer JS, et al. Cerebral blood flow changes in benign aging and cerebrovascular disease. *Neurology* 1984; 34: 855–862.